# Path Planning and Optimal Control for Autonomous Exit Parking

**Mohammad Yar-Ahmadi[1], Hamid Rahmanei[2*], Ali Ghaffari[3]**

[1]M.Sc Graduate, Mechanical Engineering, K.N.Toosi University of Technology, Tehran, Iran.

[2]Ph.D Candidate, Mechanical Engineering, K.N.Toosi University of Technology, Tehran, Iran.

[3]Professor, Mechanical Engineering, K.N.Toosi University of Technology, Tehran, Iran.

| ARTICLE INFO | A B S T R A C T |
|---|---|
| | The primary purpose of each autonomous exit parking system is to facilitate the process of exiting the vehicle, emphasizing the comfort and safety of driving in the absence of almost any human effort. In this paper, the problem of exit parking for autonomous vehicles is addressed. A nonlinear kinematic model is presented based on the geometric relationship of the vehicle velocities, and a linear time-varying discrete-time model of the vehicle is obtained for utilizing the optimal control strategy. The proposed path planning algorithm is based on the minimization of a geometric cost function. This algorithm works for ample space exit parking in Single-Maneuver and tight spaces in Multi-Maneuver exit parking. Finally, an optimal discrete-time linear quadratic control approach is hired to minimize a quadratic cost function. To evaluate the performance of the proposed algorithm, the control system is simulated by MATLAB/Simulink software. The results show that the optimal control strategy is well able to design and follow the desired path in each of the exit parking maneuvers. |

## 1. Introduction

Nowadays, with the development of cities, population growth, and ever-increasing interest of people in vehicles, the number of vehicles is increasing. Hence, parking issues in crowded and highly traveled places are becoming an overwhelming and exhausting challenge. The problems associated with the parking task may cause traffic violations and accidents. Therefore, utilizing an Autonomous Parking System (APS) is such an inevitable necessity that every driver should encounter it every day. APS provides safety and comfort, and accelerates the parking task. Unlike automatic parking systems that the driver should control acceleration/brake to park the vehicle, the advantage of the APS is that it can be used without interference from the driver.

Any APS process can be categorized into three parts, including environment perception, path planning, and tracking using a control strategy. Generally speaking, there are three types of parking, including parallel, vertical and oblique. Also, planning in autonomous vehicles can be categorized into four classes. Route planning is related to finding the best global route between the initial and final positions of motion. Path planning is considered in finding a collision-free geometric path from an initial position to a final position while traveling in the route, regarding the rules of traffic as well. The maneuver planning takes into account the path generated from path planning and takes the best high-level decision. Trajectory planning is in connection

*Corresponding Author
Email Address: hrahmanei@mail.kntu.ac.ir
http://doi.org/10.22068/ase.2023.624

with real-time planning, which is parameterized by time as well as velocity and acceleration [1]. It can exist many feasible paths, but we often require the shortest path in length.

Interpolating strategies are widely considered in the planning problems for parking. These algorithms generate the desired path based on given control points. It is shown that the shortest feasible path can be generated using circles and straight-line segments. This algorithm is applied to park in the narrow spaces in [2]. Also, a path planning strategy composed of two circular arcs connected by a tangential point is presented in [3]. Although these methods are helpful for parking in tight spaces, they generate discontinuous paths. In a discontinuous path, the steering wheel can be rotated while the velocity is zero, which leads to exhaustion of tires in the long term and puts pressure on the steering wheel. Therefore, it is an important issue that should be considered if the parking spot is long enough. To address this issue, various methods are proposed to generate a continuous path. Bezier curve fitting method build up a smooth path is applied in [4]. Also, the B-Spline curve for non-holonomic wheeled vehicles is presented in [5]. The disadvantage of this method is that the continuity gained more attention than the fitting, although it needs less collision-free area than the continuous paths created from arcs. Utilizing the circular arcs to park in tight spots is presented in [6]. After designing circular arcs, the path is transformed into a continuous form using Clothoid curves. Although a continuous path for tight parking spaces is designed, computations take time because of the integrals initiated from the clothoid curve. Reference [7] proposed a fifth-degree polynomial curve for autonomous parallel parking. A benefit of the proposed curve is that it has a low computational cost, suitable for comfort, and independent of global waypoints.

Sampling-based strategies (SBS) have largely been used in robotic applications. In some SBS, planning is based on randomly sampling configuration space and finding connectivity inside this space. One of the common algorithms of SBS, which is also applied in parking, is Rapidly-exploring Random Tree (RRT). It is a fast and probabilistic algorithm that first creates

the random tree and then chooses a path in a random way [8]. This algorithm generates discontinuous paths; besides, by taking into account that the chosen path is randomly selected and may not be optimal or suboptimal, another method is needed to improve RRT. Another strategy that may cause a non-optimal path is Hybrid A*. In order to enhance Hybrid A* algorithm, [9] proposed a method combining the Jump point search algorithm with it, which resulted in less computational time by avoiding redundant searches.

Another approach that is frequently used is Optimization-based path planning strategy (OBS). References [10] and [11] presented OBS emphasizing narrow spaces. The motivation for the use of OBS is that many constraints that are difficult to deal with in other strategies are involved in the optimization process. The process of OBS is based on the minimization of an objective function concerning problem constraints in order to find a feasible and appropriate path. If all of the constraints are satisfied simultaneously, the problem is called feasible; otherwise, it is called infeasible.

Various methods have been investigated in the literature for tracking problems in APS. A wide range of research concentrates on heuristic methods, like Fuzzy [12], Fuzzy-PID [13], and ANFIS-FCM clustering [7]. Even though these methods might guarantee robustness, they have been restricted to the knowledge of experts and are not applicable for tight parking spaces. Another obstruction concept arises in generalizing these methods. There are some constructive approaches to overcome these restrictions. Among them is the sliding mode control as an effective and robust method. It is a suitable controller to deal with a wide range of nonlinear systems and parameter uncertainties, but chattering may occur; in addition, the control law is discontinuous. An improved SMC for autonomous parking is proposed in [14], which smooths SMC output and removes high-frequency oscillations.

Model predictive control (MPC) is another valuable strategy for tracking problems, which is widely applied in literature, as in [15], [16]. The MPC method can deal with soft and hard

constraints in a multivariable control framework and provide good stability properties. However, MPC suffers from the computational burden, which hinders one from utilizing this method.

The contributions of this paper are summarized threefold. Firstly, a complete autonomous parallel exit parking algorithm based on optimization is proposed. The proposed method is developed for both large and narrow parking spaces. If there is enough space in the proposed algorithm, the vehicle will exit with only one maneuver (Single-Maneuver). Otherwise, it exits with several forward and backward moves (Multi-Maneuver Exit Parking). In the first maneuver, a number of fifth-degree polynomials are produced based on fixed initial points and variant final points among which only the one that has a minimum length and satisfies the problem constraint would be accepted. Also, in order to achieve the goal of path planning in tight spaces, the multi-maneuver exit parking is proposed which benefits from the simple geometric constraints to determine the appropriate path. Another advantage of the proposed algorithm is that it takes into account the driver or passenger comfort at the beginning of the movement. To fulfill this purpose, a smooth reference velocity is designed in such a way that increases and decreases the velocity gradually. Secondly, a new obstacle avoidance method is proposed. This method not only guarantees collision-free motion of the vehicle, but even if the obstacle width is about a motorcycle in size, the proposed method still works flawlessly. Finally, a discrete-time linear quadratic tracking (dLQT) strategy is presented to track the desired path with stability and a fast convergence rate. Also, a number of simulations in Matlab-R2019b are presented to illustrate the effectiveness of the proposed algorithm.

The rest of the paper is organized as follows. Section 2 addresses the nonlinear kinematic model of the vehicle. First, the kinematic model is presented. Then it is linearized about a reference trajectory, and the linear time-varying discrete state space model of the system is obtained. In section 3, path planning for the autonomous exit parking is presented. Two kinds of exit parking, including Single-

Maneuver and Multi-Maneuver are discussed, and a novel geometric strategy is presented for each of them. The tracking strategy based on the discrete linear-quadratic (dLQT) control is presented in section 4. In section 5, four scenarios of exit parking, including wide enough and tight Single-Maneuver and wide enough and tight Multi-Maneuver, are utilized to demonstrate the effectiveness of the proposed path planning and control strategy. Finally, conclusions are provided in section 6.

## 2. Kinematic Model

Without considering the forces that affecting the motion of the vehicle, a kinematic model based on geometry relationships of velocities can be obtained as in Figure 1. Because the vehicle exits from parking in low speed, the slip angle of the wheels is negligible. Defining state vector as $X = [x, y, \theta]^T$ and input vector as $U = [v, \phi]^T$, the kinematic model of the vehicle is

$$dX/dt = F(X,U)$$
$$[\dot{x}, \dot{y}, \dot{\theta}]^T = [v\cos\theta, v\sin\theta, v\tan\phi/L]^T \quad (1)$$

Where $O$ is the instantaneous center of rotation; $(x, y)$ coordinates are placed at the center of the rear axle; $\theta$ is the heading angle; $v$ is longitudinal velocity; $\phi$ is the steering angle, and $L$ is the distance between the front and rear axles known as wheelbase.

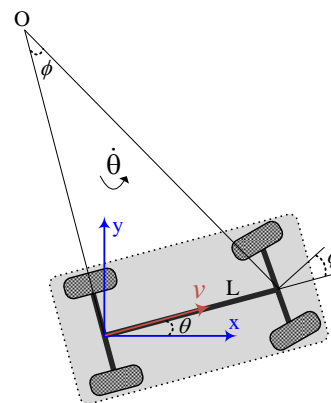The kinematic model presented in Figure (1) is



**Figure 1:** Kinematic model of the vehicle.

hired to extract a nonlinear system in (1), so it cannot be utilized to design the linear optimal controller. Therefore, it is linearized around a reference trajectory $(X_{ref}, Y_{ref})$, and then discretized. The following equation governs the reference trajectory

$$dX_{ref}/dt = F(X_{ref}, U_{ref}) \qquad (2)$$

Now, expanding the right-hand side of (1) around the reference trajectory in (2), ignoring the higher-order terms, gives

$$
\begin{aligned}
F(X, U) \approx & F(X_{ref}, U_{ref}) \\
& + (\partial F/\partial X)|_{\substack{X_{ref}\\U_{ref}}}(X - X_{ref}) \\
& + (\partial F/\partial U)|_{\substack{X_{ref}\\U_{ref}}}(U - U_{ref})
\end{aligned} \qquad (3)
$$

In following, combining the Equations (1) to (3), gives

$$
\begin{aligned}
d\tilde{x}/dt = & (\partial F/\partial X|_{\substack{X_{ref}\\U_{ref}}})\tilde{x} \\
& + (\partial F/\partial U|_{\substack{X_{ref}\\U_{ref}}})\tilde{u}
\end{aligned} \qquad (4)
$$

Where, $\tilde{x} = X - X_{ref}$ and $\tilde{u} = U - U_{ref}$. Finally, utilizing the forward discretization of Euler method with sampling time $T$ and some matrix manipulation gives the linearized discrete-time state model as

$$
\begin{aligned}
&\tilde{x}_{k+1} = A_k \tilde{x}_k + B_k \tilde{u}_k, \\
&A_k = \begin{bmatrix} 1 & 0 & -Tv_{ref,k}\sin\theta_{ref,k} \\ 0 & 1 & Tv_{ref,k}\cos\theta_{ref,k} \\ 0 & 0 & 1 \end{bmatrix} \\
&B_k \\
&= \begin{bmatrix} T\cos\theta_{ref,k} & 0 \\ T\sin\theta_{ref,k} & 0 \\ T\tan\phi_{ref,k}/L & Tv_{ref,k}/(L\cos^2\phi_{ref,k}) \end{bmatrix}
\end{aligned} \qquad (5)
$$

## 3. Path Planning

In terms of environmental information, path planning for the APS can be divided into global

and local categories. The former assumes environmental information is known, and the latter assumes not. In this research, global path planning is considered for two cases. In the first case, named as Single-Maneuver, the space is large enough, and the exiting process can be done with one maneuver. In the second case, named as Multi-Maneuver, the space is so tight that the exiting process needs at least two forward and backward moves. In the following, the proposed approaches for both of them are presented.

### 3.1. Single-Maneuver Exit Parking

In this part, a number of the fifth-degree polynomials are produced based on fixed initial points $(x_i, y_i)$ and variant final points $(x_f, y_f)$. Among these paths, only the one that has a minimum length and satisfies the problem constraint, $g_j$, would be accepted. For this purpose, the following cost function is proposed

$$J = \min \ \|Length\ of\ the\ curve\|$$

$$s.t. \begin{cases} g_1: \text{Collision avoidance constraints} \\ g_2: \text{Enter to opposite lane avoidance} \\ g_3: \text{Steering angle constraint} \end{cases} \qquad (6)$$

A fifth-degree polynomial is a continuous path; the velocity of the vehicle does not reach to zero while traversing the path. It has the following properties

$$\text{Initial: } y(x_i) = y_i, \begin{cases} dy(x_i)/dx = 0 \\ d^2y(x_i)/dx^2 = s \end{cases} \qquad (7)$$

$$\text{Final: } y(x_f) = y_f, \begin{cases} dy(x_f)/dx = 0 \\ d^2y(x_f)/dx^2 = 0 \end{cases} \qquad (8)$$

Where the constant $s$ is obtained regarding the initial desired steering angle. The fifth-degree polynomial describing the path is as follows

$$y(x) = \sum_{n=0}^{n=5} a_n x^n \qquad (9)$$

Where coefficients $a_j, j = 1, \dots, 5$ are obtained as follows

$$\begin{bmatrix} a_0 \\ a_1 \\ a_2 \\ a_3 \\ a_4 \\ a_5 \end{bmatrix}$$

$$= \begin{bmatrix} 1 & x_i & x_i^2 & x_i^3 & x_i^4 & x_i^5 \\ 1 & x_f & x_f^2 & x_f^3 & x_f^4 & x_f^5 \\ 0 & 1 & 2x_i & 3x_i^2 & 4x_i^3 & 5x_i^4 \\ 0 & 1 & 2x_f & 3x_f^2 & 4x_f^3 & 5x_f^4 \\ 0 & 0 & 2 & 6x_i & 12x_i^2 & 20x_i^3 \\ 0 & 0 & 2 & 6x_f & 12x_f^2 & 20x_f^3 \end{bmatrix} \begin{bmatrix} y_i \\ y_f \\ 0 \\ 0 \\ s \\ 0 \end{bmatrix} \qquad (10)$$

Two components of paths generated in the fifth-degree polynomial form are discretized as

$$x_f = [x_{f,min}: (x_{f,max} - x_{f,min})/n : x_{f,max}]$$
$$y_f = [y_{f,min}: (y_{f,max} - y_{f,min})/n : y_{f,max}] \qquad (11)$$

Where $x_{f,min}$ and $x_{f,max}$ are the minimum and maximum desired longitudinal endpoints of the paths, respectively, $y_{f,min}$ and $y_{f,max}$ are the minimum and maximum desired lateral endpoints of the paths, respectively. The number of created paths is relative to the time increment, n. Increasing the number of paths (increasing $n$) can lead to increasing the probability of finding the path with lesser length; because all paths are initiated at $(x_0, y_0) = (0,0)$, and the essential difference between them is the point at which they end. Once the time increment increases, the points between the desired endpoints will be raised. More precisely, since the proposed method creates paths based on the number of endpoints, and we increased $n$, then we have more endpoints for creating more paths. As a result, the number of paths will be increased. Let us investigate an example. As in Figure 2, If $n = 6$, we have 6 final positions $(x_f, y_f)$, so the number of paths would be equal to 6*6=36 paths, regardless of the values of $x_f$ and $y_f$.

The length of each polynomial path is calculated from the following integral

$$L_P = \int_{x_i}^{x_f} \sqrt{1 + (dy/dx)^2} dx \qquad (12)$$

In order to provide driver comfort, a smooth reference velocity based on g-bell function, which smoothly starts from zero velocity, reaches a maximum desired velocity, $v_{max}$, and ends to zero velocity, is created as in (13)

$$v_{ref,k} = v_{max} G_{bell}(a, b, c, k, T)$$
$$= v_{max}/(1 + |kT - c/a|^{2b}) \qquad (13)$$

The steering and heading angle $\theta_{ref}$ and $\phi_{ref}$ are presented as in (14) and (15), respectively
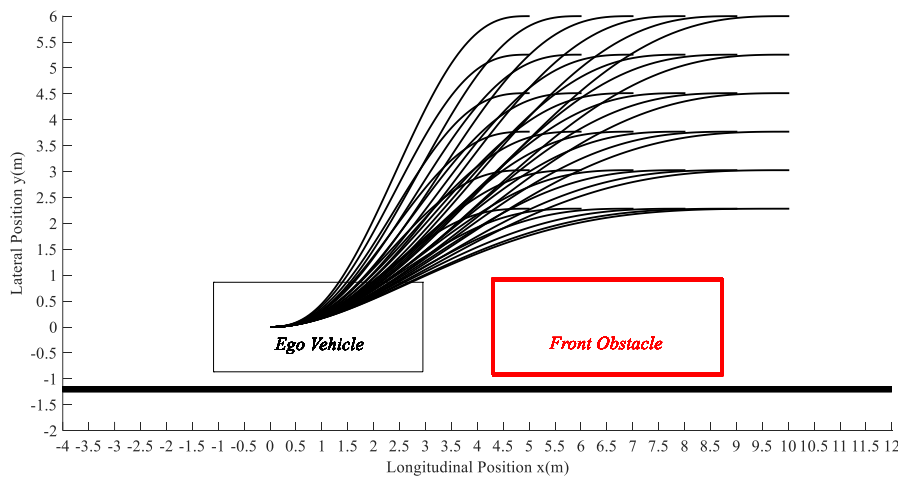


**Figure 2:** The number of created paths is based on the number of endpoints $n$. In this example, $n = 6$ which results in 36 created paths.

$$\theta_{ref,k} = \tan^{-1}(dy/dx) \tag{14}$$

$$v_{ref,k} = \tan^{-1}(L\frac{d^2y/dx^2}{[1+(dy/dx)^2]^{3/2}}) \tag{15}$$

Using geometric relations can easily obtain horizontal and vertical coordinates for each corner of the vehicle in Figure 3. For instance, $x_{fr}$ and $y_{fr}$ coordinates for the front right corner of the vehicle in Figure 3 are

$$\begin{bmatrix} x_{fr} \\ y_{fr} \end{bmatrix} = \begin{bmatrix} x \\ y \end{bmatrix} + \begin{bmatrix} L + L_f \\ -(W/2 + W_f) \end{bmatrix}\cos\theta + \begin{bmatrix} W/2 + W_f \\ L + L_f \end{bmatrix}\sin\theta \tag{16}$$

The coordinates for the other three corners of the autonomous vehicle can be obtained similarly.

For collision-free path planning, a novel method is presented. In this method, coordinates of each important corner of the obstacles are calculated relative to connected local coordinate systems at the corners of the vehicle. If an important corner of the obstacles enters the forbidden quarter of a coordinate system, the path will be omitted.

In Single-Maneuver exit parking, the local coordinate system $O_1$ is placed at the front right corner of the vehicle in Figure 3. For exit parking without collision, the corner A should not enter the second quarter of the local coordinate system $O_1$. Therefore, the first, third, and fourth quarters of $O_1$ are admissible regions, as shown in Figure 4-a and 4-b. As a result, the front and the right edges of the vehicle, which is
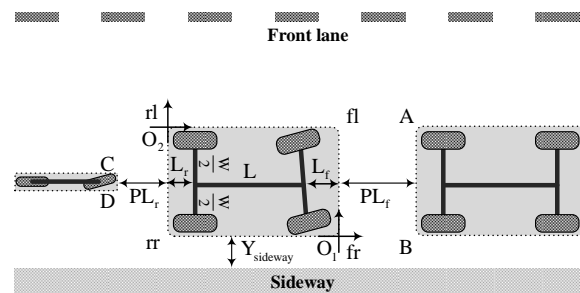


**Figure 3:** Illustration of Exit Parking Scenario.

the most crucial boundary in the Single-Maneuver exit parking problem, remain without collision. This constraint is expressed as in (17)

$$\begin{cases} CP_1 = \begin{bmatrix} \cos\theta & -\sin\theta \\ \sin\theta & \cos\theta \end{bmatrix}\begin{bmatrix} x_A - x_{fr} \\ y_A - y_{fr} \end{bmatrix} \\ [CP_1]_{1\times1} > 0 \ or \ [CP_1]_{2\times1} < 0 \end{cases} \tag{17}$$

Consequently, the objective function associated with these constraints can be rewritten as

$$J = \min \ \{L_P\}$$
$$s.t.\begin{cases} [CP]_{1\times1} > 0 \ or \ [CP]_{2\times1} < 0 \\ y_{fr,k} < y_{Opposite\ lane} \\ \phi_k < \phi_{max} \end{cases} \tag{18}$$

### 3.2. Multi-Maneuver Parking

When the vehicle is parked in a tight space, the driver steers with the maximum steering angle to the left and moves forward until the vehicle reaches the front obstacle. Then, the driver steers with the maximum steering angle to the right and moves backward until the vehicle
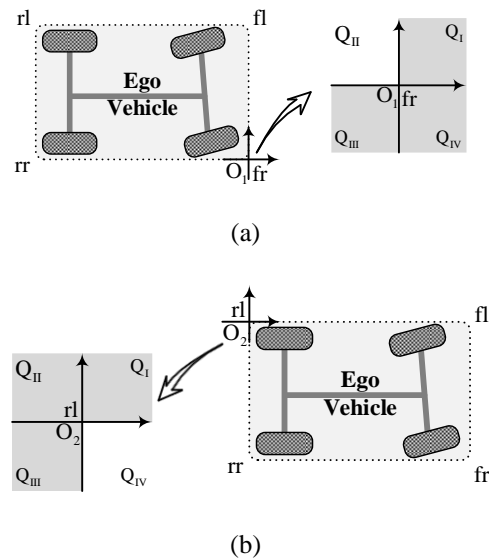


(a)



(b)

**Figure 4:** Illustration of (a) $CP_1$ and (b) $CP_2$ constraints. Shaded quarters show admissible regions in the local coordinate systems, O1 and O2. By using CP1 and CP2, the ego vehicle keeps without collison with the front and the rear obstacles, respectively.

reaches the rear or side obstacles. This process continues until the front right corner of the vehicle moves upper than the point A, as in Figure 3. As soon as this happened, any kind of curve can be used in order to exit all parts of the vehicle from the parking. Consequently, this paper only focused on exiting the front part of the vehicle in Multi-Maneuver exit parking.

The path consists of circular arcs with minimum radius and maximum steering angle. Equations of each move are

$$
\begin{aligned}
X &= x_0 - R_{min}\sin\theta \\
Y &= y_0 - R_{min}\cos\theta \\
\theta &= \theta_0 + d\operatorname{sgn}(R_{min}D) \\
R_{min} &= L/\tan\phi_{max}
\end{aligned}
\tag{19}
$$

Where the parameter $D$ is equal to $+1$ for a forward move and is equal to $-1$ for a backward move; the parameter $d$ is the variation of the tangent line to the last created curve. Obstacle avoidance constraints, in this case, are formulated as (20), (21), and (22).

$$
\begin{aligned}
&a\colon\ Y_v > -\left(W/2 + W_r + Y_{sideway}\right) \\
&b\colon\ \begin{cases} -(L_r + PL_r) < X_v < \left(L + L_f + PL_f\right) \\ \text{or}\ \ Y_v > y_A \\ \text{or}\ \ Y_v > y_C \end{cases} \\
&c\colon\ y_{fr} < y_A + y_{Th}
\end{aligned}
\tag{20}
$$

Where $(X_v, Y_v)$ are the coordinates of the four corners of the vehicle, $v \in \{fl, fr, rl, rr\}$; $W_f$ and $W_r$ are the lateral distance from the center of the front and the rear wheels, respectively, to the body of the ego vehicle.

The ranges of motion of the vehicle are restricted in (20). As seen in (20-a) and Figure 5-a, the vehicle must move upper than sideway. Furthermore, $X_v$ must be between the two obstacles; otherwise, $Y_v$ must be upper than the width of the obstacles, as shown in (20-b) and Figure 5-b. The last constraint in (20-c), and Figure 5-c, is the finisher of the maneuver. It means that if $y_{fr}$ is greater than $y_A$ plus a desired lateral threshold distance, which is $y_{Th} = 0.3\,m$ here, the maneuver must be stopped. As discussed before, we only focused on exiting the front part of the vehicle in Multi-Maneuver exit parking. Therefore, with this

constraint, the goal is achieved. It should be emphasized that the shaded areas in Figure 5 show allowed areas of motion of the ego vehicle by their specified constraint.

The other obstacle avoidance constraints are presented as

$$
\begin{cases} CP_1 = \begin{bmatrix} \cos\theta & -\sin\theta \\ \sin\theta & \cos\theta \end{bmatrix}\begin{bmatrix} PL_f + L_f + L - x_{fr} \\ y_B - y_{fr} \end{bmatrix} \\ [CP_1]_{1\times1} > 0\ or\ [CP_1]_{2\times1} < 0 \end{cases}
\tag{21}
$$

$$
\begin{cases} CP_2 = \begin{bmatrix} \cos\theta & -\sin\theta \\ \sin\theta & \cos\theta \end{bmatrix}\begin{bmatrix} -PL_r - L_f - x_{rl} \\ y_C - y_{rl} \end{bmatrix} \\ [CP_2]_{1\times1} < 0\ or\ [CP_2]_{2\times1} > 0 \end{cases}
\tag{22}
$$

For Multi-Maneuver exit parking, in addition to the local coordinate system $O_1$, another local coordinate system which is placed at the rear left corner of the vehicle is required. Admissible regions in this local coordinate system, which is called $O_2$, are the first, second, and third quarters, as shown in Figure 5-b. Therefore, the rear and left edges of the vehicle remain safe. Consequently, all four edges of the vehicle would have no collision with the front and rear obstacles because of constraints $CP_1$ and $CP_2$ in (21) and (22), respectively.

## 4. Control Design

The block diagram of the overall system with the optimal discrete-time linear quadratic tracking controller is shown in Figure 6. Assume given the state and output equations of a linear discrete-time system as

$$
\begin{aligned}
\tilde{x}_{k+1} &= A_k\tilde{x}_k + B_k\tilde{u}_k \\
y &= C_k\tilde{x}_k
\end{aligned}
\tag{23}
$$

And the corresponding cost function to be minimized is formulated as in (24)

$$
\begin{aligned}
J = \{ &1/2\sum_{k_0}^{kf-1}\left\|C\tilde{x}_k - z_{des,k}\right\|_{Q_k}^2 + \|\tilde{u}_k\|_{R_k}^2 \\
&+ 1/2\left\|C\tilde{x}_{kf} - z_{des,kf}\right\|_{F_k}^2 \}
\end{aligned}
\tag{24}
$$

Where the expression $\|u_k\|_{R_k}^2$ of the inputs is equal to $u_k^T R_k u_k$, and $F_k$ and $Q_k$ denote two 3×3
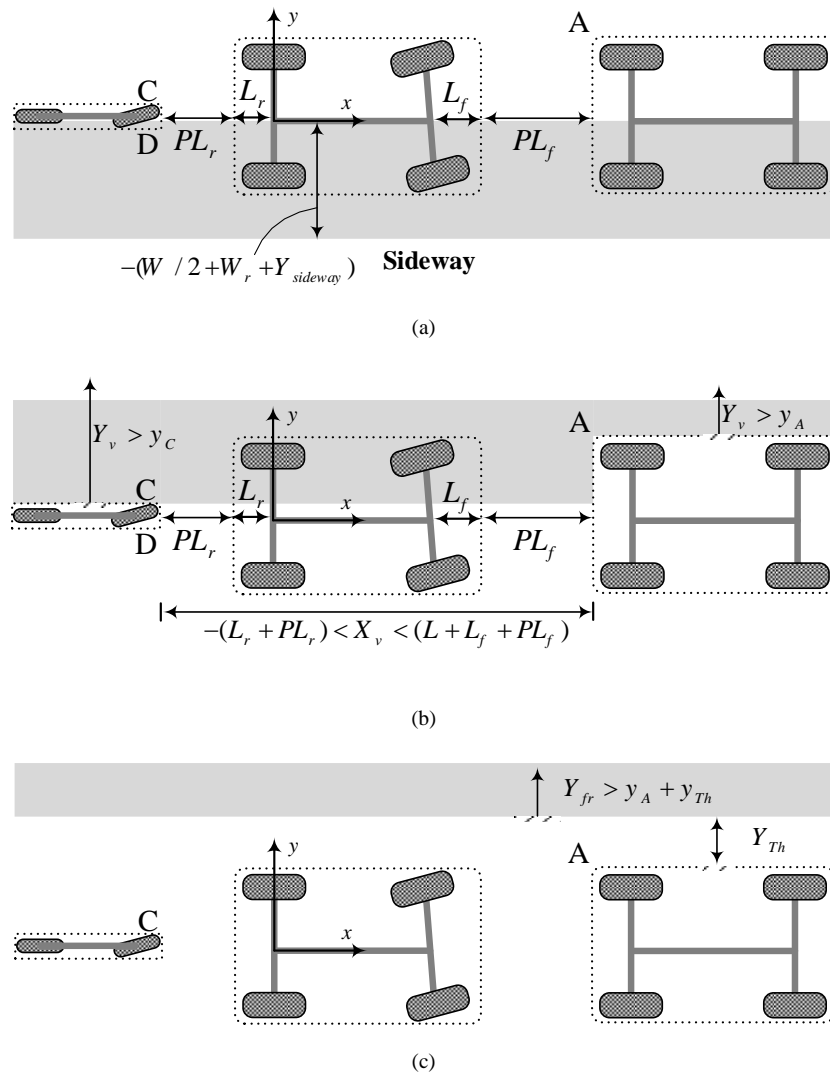
**Figure 5:** Motion restrictions of the vehicle in Multi-Maneuver exit parking scenarios. (a), (b), and (c) illustrate the constraints (20-a), (20-b), and (20-c), respectively.
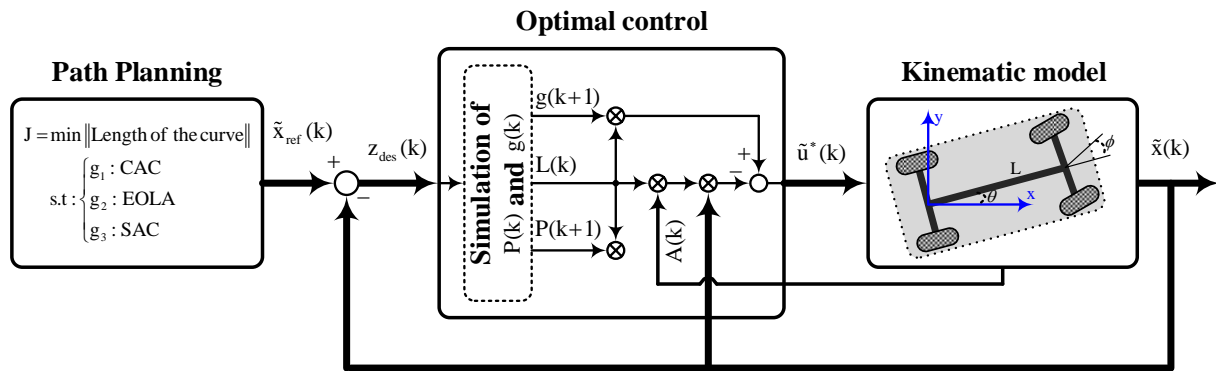


**Figure 6:** Block diagram of the overall control system, including path planning block and optimal discrete-time linear quadratic tracking (dLQT).

4069    Automotive Science and Engineering (ASE)

positive semi-definite symmetric matrices which represent the weight matrix of penalty at the final time and weight matrix of state variables, respectively. Also, $R_k$ stands for a 2×2 positive definite symmetric matrix.

In this optimal linear path tracking problem, the desired situation is that the vector $C\tilde{x}_k$ converges to $z_{des,k}$. So, the value of this error vector in the time interval between $k_0$ and $k_f$ indicates the deviation of the variables of the controlled state from the desired values. Same way, the term $C\tilde{x}_{kf} - z_{des,kf}$ indicates that the final value $C\tilde{x}_{kf}$ is how far from its desired value $z_{des,kf}$. The first term in summation of the right-hand side of (24) shows how much the control system designer cares about the deviation of states from their desired values. The larger the coefficient $Q_k$ is chosen, the smaller the tracking error is and the closer it is to zero, which yields better tracking. On the other hand, The larger the coefficient $R_k$ is chosen, the smaller the input control effort is and the closer it is to zero. It should be noted that a compromise must be established between the selected values for these weight coefficient matrices.

To solve the problem, in the first step, the following matrix difference Riccati equation with the corresponding terminal condition $P_{kf}$ is to be solved [17],

$$P_k = A_k^T P_{k+1}[I + E_k P_{k+1}]^{-1} A_k + V_k$$
$$P_{kf} = C_{kf}^T F_{kf} C_{kf} \tag{25}$$

Where, $V_k$ and $E_k$ are equal to $C_k^T Q_k C_k$ and $B_k R_k^{-1} B_k^T$, respectively.

In the second step, the vector form of the difference equation is solved

$$g_k = A_k^T \left[I - \left(P_{k+1}^{-1} + E_k\right)^{-1} E_k\right] g_{k+1} + C_k^T Q_k z_k \tag{26}$$

$$g_{kf} = C_{kf}^T F_{kf} z_{kf}$$

In the third step, the optimal states are obtained using the following equations [17],

$$L_k = \left[R_k + B_k^T P_{k+1} B_k\right]^{-1} B_k^T$$
$$\tilde{x}_{k+1}^* = A_k \tilde{x}_k^* - B_k L_k[\tilde{x}^* - g_{k+1}] \tag{27}$$

Finally, in the fourth step, the optimal control input is obtained

$$\tilde{u}_k^* = -L_k[P_{k+1} A_k \tilde{x}_k^* - g_{k+1}] \tag{28}$$

## 5. Simulation Results and Discussion

In order to verify the effectiveness of the proposed algorithm, four exit parking scenarios are studied in MATLAB/Simulink. The first two scenarios are for the cases that the parking spaces are adequate to exit the vehicle from the parking area with one maneuver. In comparison, the second two scenarios are for the condition that the parking space is tight. As a result, the vehicle must exit from the parking area with multiple forward and backward moves.

The geometric parameters of the vehicle used for the simulation, including wheelbase, track width, front and rear overhang distances, maximum steering angle, and maximum distance from sideway to opposite lane are presented in Table 1. Moreover, the values of the geometric parameters related to the parking areas are given in Table 2.

### 5.1. First two Scenarios (Single-Maneuver)

In the first scenario of this case, the length and width of the parking space are nearly short, but it is sufficient to exit the vehicle from parking with a single maneuver. Furthermore, all of the vehicles are parked in the same direction.

The simulation results of the reference and actual outputs, including the lateral position of the center of the rear axle $y(t)$, and the heading angle $\theta(t)$, are provided in Figure 7.

As shown in Figure 7, one can see that the proposed method can track the reference outputs accurately. The reference outputs are calculated by minimization of the performance index in (6).

**Path Planning and Optimal Control for Autonomous Exit Parking**

**Table 1:** List of the vehicle parameters.

| Symbol | Quantity Description | Values |
|---|---|---|
| $L$ | Wheelbase | 2.35 m |
| $W$ | Track width | 0.764 m |
| $L_f$ | Front overhang | 0.6 m |
| $L_r$ | Rear overhang | 1.1 m |
| $W_f$ | Lateral distance from the front wheels to the side edges of the vehicle | 0.1 m |
| $W_r$ | Lateral distance from the rear wheels to the side edges of the vehicle | 0.1 m |
| $\phi_{max}$ | Maximum steering angle | 48.5 º |
| $v_{max}$ | Maximum longitudinal velocity for the first and second scenario, respectively | 0.694 m/s 0.84 m/s |
| $Y_{opposite\ lane}$ | Lateral distance from sideway to the opposite lane | 5.25 m |

**Table 2:** List of the parking area parameters.

| Parking area parameters | Scenarios | | | |
|---|---|---|---|---|
| | Wide enough (1) | Wide enough (2) | Tight (3) | Tight (4) |
| $PL_f$ | 1.35 m | 1.5 m | 0.5 m | 0.2 m |
| $P_r$ | 0.1 m | 0.1 m | 0.3 m | 0.3 m |
| $Y_{sideway}$ | 0.336 m | 0.336 m | 0.4 m | 0.4 m |
| $x_A$ | 4.3 m | 4.45 m | 3.15 m | 3.15 m |
| $y_A$ | 0.92 m | 1.32 m | 0.4 m | 0.6 m |
| $x_B$ | 4.3 m | 4.45 m | 3.45 m | 3.15 m |
| $y_B$ | -0.92 m | -0.52 m | -0.4 m | -0.2 m |
| $x_C$ | -1.19 m | -1.19 m | -1.39 m | -1.39 m |
| $y_C$ | 0.92 m | 0.92 m | 0.4 m | -0.1 m |
| $x_D$ | -1.19 m | -1.19 m | -1.39 m | -1.39 m |
| $y_D$ | -0.92 m | -0.92 m | -0.4 m | -0.9 m |

Considering the geometric constraints for collision avoidance, together with endpoints of the path, provides numbers of admissible paths, and the one with the shortest length is chosen. Then using the reference values in (13) to (15), and in collaboration with optimal control $\tilde{u}_k^*$ in (28), the task of tracking is done perfectly. It is noteworthy that the control input makes the system to follow the desired outputs while minimizing the performance index in (24). The optimal control inputs $v$ and $\phi$ in comparison with reference inputs are shown in Figure 8.

The results of the two outputs and the two control inputs for the second scenario are shown in Figure 9. As can be seen in Figure 9, the output tracking and optimal control input generation are also provided for this scenario ideally. The core difference between the

scenarios one and two is that in the second scenario, the position of the front obstacle is modified to create a tighter and more complex space for the ego vehicle. However, the proposed method works well in this scenario like the previous one, as seen in Figure 9.

The dynamic process of exit parking of the vehicle in Single-Maneuver exit parking for the first two scenarios is shown in Figure 10. As can be seen, the object avoidance task is done perfectly in both scenarios.

**5.2. Second two Scenarios (Multi-Maneuver)**

The vehicle in these two cases cannot exit from the parking with one simple maneuver. Since the space is limited, the Single-Maneuver
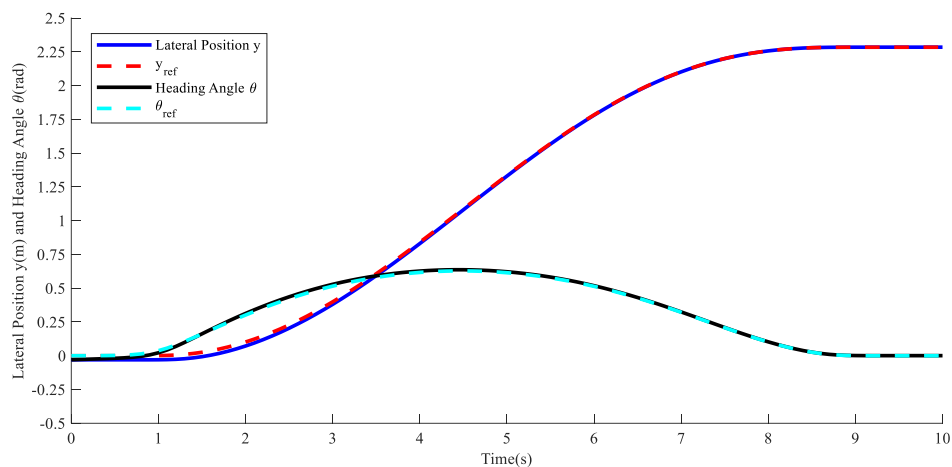
(b)

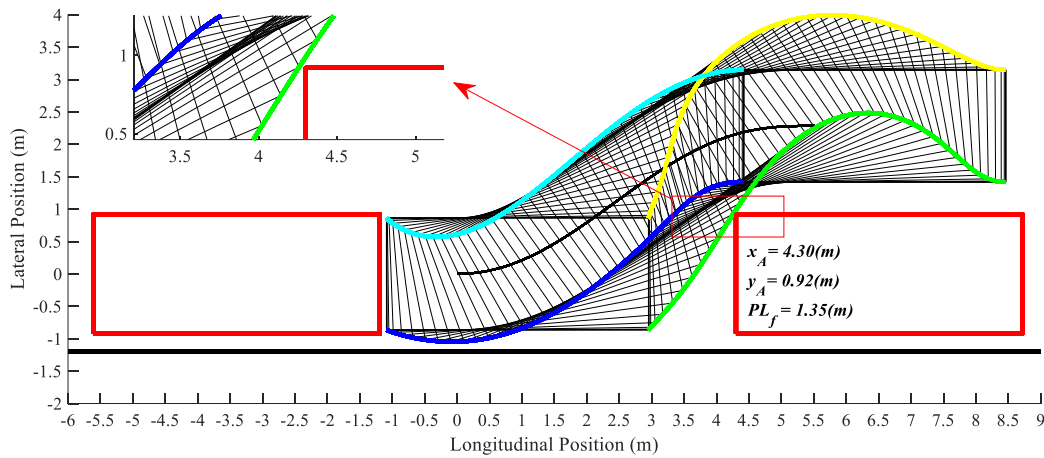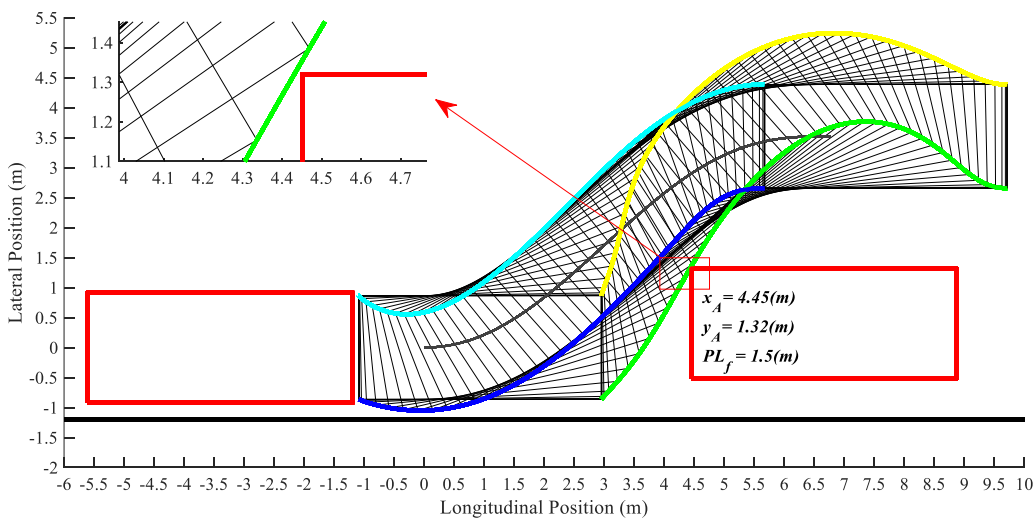**Figure 9:** Simulation of Single-Maneuver exit parking, for the second scenario. (a) Reference and actual outputs. (b) The optimal control inputs.



(a)



(b)

**Fig. 10.** The dynamic process of exit parking of the vehicle in Single-Maneuver exit parking, (a) First scenario, (b) Second scenario. The subfigures show magnifying picture of vital areas of the exit parking scenario.

method cannot find an admissible path that satisfies the geometric constraints and exit the vehicle from parking with one continuous path. Therefore, the Multi-Maneuver method is applied. Thus, a complete approach for exit parking is provided here.

To the author's best knowledge, in most of the articles, the width of obstacles is approximately considered to be the same width of the vehicle or more than it; whereas in real-world scenarios, there might be obstacles with less width, like a motorcycle. In such cases, no collision with the left corner of the back obstacle and the right corner of the front obstacle becomes more critical. In the presented method, the width of

the obstacles is considered as small as a motorcycle width in order to overcome this issue. As we can see in Figure 11-a, despite the limited and tight parking space, the vehicle exit from the parking without any collision by series of forward and backward moves.

The critical difference between the scenarios one and two is that in the latter scenario, the positions of the front and rear obstacles are changed due to creating a tighter and more complex space for the ego vehicle. However, we can see that the proposed method works well in this scenario, as well as the previous one, as shown in Figure 11-b.
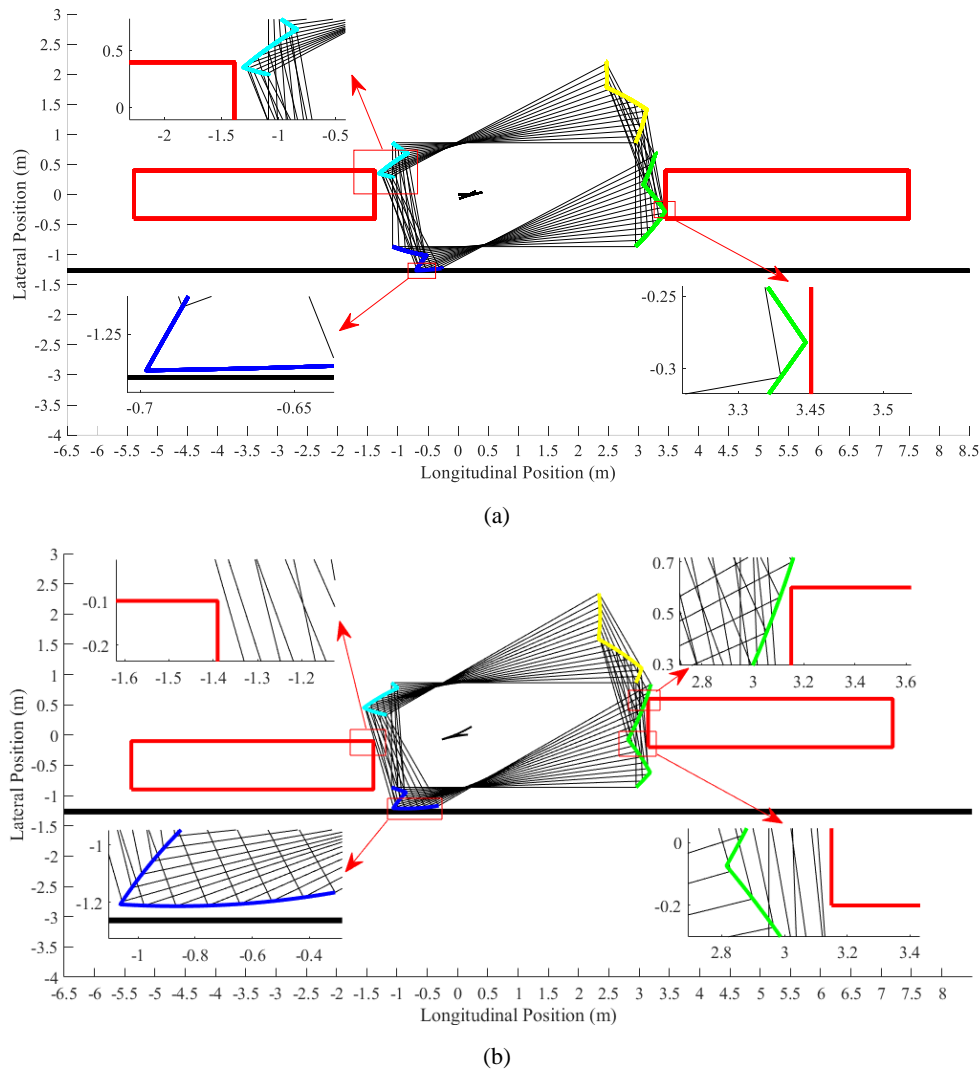


(a)



(b)

**Fig. 11.** The dynamic process of Multi-Maneuver exit parking, for (a) First scenario, (b) Second scenario. The front part of the vehicle exit from parking successfully and without any collision. The subfigures show magnifying picture of vital areas of the exit parking scenario.

## 6. Conclusions

In this research, a novel and complete path planning approach (as it can be used for both wide and narrow spaces), based on minimization of the cost function (which selects the shortest generated path considering the constraints of collision avoidance), and an optimal discrete-time linear quadratic control with finite horizon is presented. Our studies showed that the proposed method is able to perform the autonomous exit parking task with both wide and narrow spaces by utilizing Single-Maneuver, which uses a continuous and smooth path, or Multi-Maneuver, which uses minimum radius circular arcs. Moreover, in order to achieve driver or passenger comfort at the beginning of the movement, a smooth reference velocity based on a g-bell function, which increases and decreases the velocity gradually, is provided. The proposed path planning method guarantees collision-free motion of the vehicle through the mathematical and geometrical constraints. Additionally, it works well for obstacles that have a smaller size than a sedan vehicle, for instance, a motorcycle.

In the end, the simulation results verified the effectiveness of our suggested approach. This research work can be enriched by experimental implementations, which is our future work.

## Declaration of Conflicting Interests

The author(s) declared no potential conflicts of interest with respect to the research, authorship, and/or publication of this article.

## References

[1] C. Katrakazas, M. Quddus, W. Chen, L. Deka., Real-time motion planning methods for autonomous on-road driving: State-of-the-art and future research directions, J. Transportation Research Part C: Emerging Technologies, Vol. 60, (2015), pp. 416–442.

[2] Z. Lv, L. Zhao, and Z. Liu, A path-planning algorithm for automatic parallel parking, IMCCC, China, (2013), pp. 474-478.

[3] X. Ji, J. Wang, Y. Zhao, Y. Liu, L. Zang & B. Li, Path planning and tracking for vehicle parallel parking based on preview BP neural network PID controller, Trans. Tianjin University, Vol. 21, (2015), pp. 199-208.

[4] Z. Liang, G. Zheng, and J. Li, Automatic parking path optimization based on Bezier curve fitting, ICAL, China, (2012), pp. 583–587.

[5] F. Gómez-Bravo, F. Cuesta, A. Ollero, and A. Viguria, Continuous curvature path generation based on β-spline curves for parking manoeuvres, J. Robotic Autonomous Systems, Vol. 56, No. 4, (2008), pp. 360–372.

[6] H. Vorobieva, S. Glaser, N. Minoiu-Enache, S. Mammar Automatic parallel parking in tiny spots: Path planning and control, IEEE Transactions Intelligent Transportation Systems, Vol. 16, No. 1, (2015), pp. 396–410.

[7] H. Rezaei Nedamani, P. Masnadi Khiabani, and S. Azadi, Intelligent parallel parking using adaptive neuro-fuzzy inference system based on fuzzy c-means clustering algorithm, SAE Technical Papers, (2017).

[8] B. Lee, Y. Wei, and I. Y. Guo, Automatic parking of self-driving car based on LiDAR, Int. Arch. Photo., Rem. Sens. Spat. Inf. Sci. - ISPRS Archives, Vol. 42, (2017), pp. 241–246.

[9] Z. Qin, X. Chen, M. Hu, L. Chen, J. Fan, A novel path planning methodology for automated valet parking based on directional graph search and geometry curve, J. Robotic Autonomous Systems, Vol. 132, (2020).

[10] L. Cai, H. Guan, H. L. Zhang, X. Jia, J. Zhan, "Multi-maneuver vertical parking path planning and control in a narrow space," J. Autonomous Systems, Vol. 149, ( 2022).

[11] P. Zips, M. Böck, A. Kugi, Optimisation based path planning for car parking in narrow environments, J. Robotic Autonomous Systems, Vol. 79, (2016).

[12] W. Yang, L. Zheng, Y. Li, Y. Ren, and Y. Li, A trajectory planning and fuzzy control for

autonomous intelligent parking system, SAE Technical Papers, (2017).

[13] E. Ballinas, O. Montiel, O. Castillo, Y. Rubio, and Aguilar, A., Automatic parallel parking algorithm for a car-like robot using fuzzy pd+i control, Engineering Letters, Vol. 26, No. 4, (2018), pp. 447-454.

[14] X. Du and K. K. Tan, Autonomous reverse parking system based on robust path generation and improved sliding mode control, IEEE Transactions on Intelligent Transportation Systems, Vol. 16, No. 3, (2015), pp. 1225–1237.

[15] H. Ye, H. Jiang, S. Ma, B. Tang, and L. Wahab, "Linear model predictive control of automatic parking path tracking with soft constraints," Int. J. Advanced Robotic Systems, Vol. 16, No. 3, (2019) , pp. 1–13.

[16] C. Ma, F. Li, C. Liao, and L. Wang, Path following based on model predictive control for automatic parking system, SAE Technical Papers, (2017).

[17] A. Ghaffari, A. Khodayari, F. C. Samavati, Advanced control and dynamic systems. K.N.T.U Press, Tehran, Iran (2020). (In Persian)